

## Size-Expanded yDNA Bases: An Ab Initio Study

M. Fuentes-Cabrera,<sup>\*,†</sup> Bobby G. Sumpter,<sup>†</sup> Pawel Lipkowski,<sup>‡</sup> and Jack C. Wells<sup>†</sup>

Center for Nanophase Materials Sciences, and Computer Science and Mathematics Division,  
Oak Ridge National Laboratory, P.O. Box 2008, Oak Ridge, Tennessee 37831-6494, and  
Institute of Physical and Theoretical Chemistry, Wrocław University of Technology,  
Wybrzeże Wyspiańskiego 27, 50-379 Wrocław, Poland

Received: December 16, 2005; In Final Form: January 25, 2006

xDNA and yDNA are new classes of synthetic nucleic acids characterized by having base-pairs with one of the bases larger than the natural congeners. Here these larger bases are called x- and y-bases. We recently investigated and reported the structural and electronic properties of the x-bases (Fuentes-Cabrera et al. *J. Phys. Chem. B* 2005, 109, 21135–21139). Here we extend this study by investigating the structure and electronic properties of the y-bases. These studies are framed within our interest that xDNA and yDNA could function as nanowires, for they could have smaller HOMO–LUMO gaps than natural DNA. The limited amount of experimental structural data in these synthetic duplexes makes it necessary to first understand smaller models and, subsequently, to use that information to build larger models. In this paper, we report the results on the chemical and electronic structure of the y-bases. In particular, we predict that the y-bases have smaller HOMO–LUMO gaps than their natural congeners, which is an encouraging result for it indicates that yDNA could have a smaller HOMO–LUMO gap than natural DNA. Also, we predict that the y-bases are less planar than the natural ones. Particularly interesting are our results corresponding to yG. Our studies show that yG is unstable because it is less aromatic and has a Coulombic repulsion that involves the amino group, as compared with a more stable tautomer. However, yG has a very small HOMO–LUMO gap, the smallest of all the size-expanded bases we have considered. The results of this study provide useful information that may allow the synthesis of an yG-mimic that is stable and has a small HOMO–LUMO gap.

## Introduction

During the past few years, Kool and co-workers have synthesized size-expanded DNA bases, which are characterized by being a fusion between a natural base (A, C, G and T; Figure 1) and a benzene ring. Currently, there are two types of size-expanded bases, the x-bases<sup>1a,b,c</sup> (xA, xC, xG and xT; Figure 2) and the y-bases<sup>2a,b</sup> (yA, yC, yT, and yT-methyl; Figure 3). Both types have been combined with natural bases to form the synthetic nucleic acids known as xDNA<sup>1d–g</sup> and yDNA.<sup>2a,c</sup> Both x- and y-bases are potentially useful for developing biosensor assays and for probing how steric changes affect protein–DNA interactions. For example, recently Kool and co-workers have used several T analogues, which are characterized by being larger in size than T, to gain insight into the DNA replication process.<sup>3</sup>

We believe that xDNA and yDNA could also have nanotechnological applications. On one hand, it may be possible to build nanostructures made of these duplexes. This is because xDNA and yDNA preserve, at least at some level, DNA's recognition property. For example, experiments have shown that xA<sup>1f</sup> and yA<sup>2a</sup> prefer binding to T. Since the recognition property has been used to assemble nanostructures made of natural DNA,<sup>4</sup> one can envision nanostructures made of xDNA or yDNA. On the other hand, these duplexes could function as nanowires. The logic here is that the HOMO–LUMO gaps of xDNA and yDNA might be smaller than those of natural DNA.

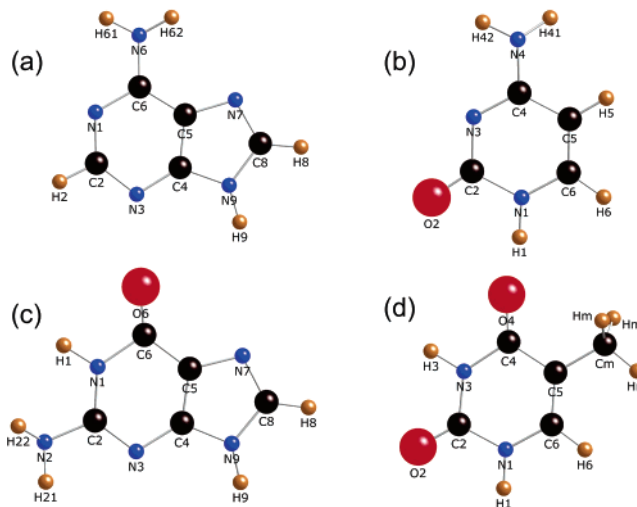


**Figure 1.** Natural DNA bases: (a) adenine, A; (b) cytosine, C; (c) guanine, G; (d) thymine, T. Color code: oxygen, red; carbon, black; nitrogen, blue; hydrogen, maroon.

We recently investigated the electronic properties of xA, xC, xG, xT, A, C, G, and T and found that the x-bases have smaller HOMO–LUMO gaps than the natural bases.<sup>5</sup> Furthermore, Kool and co-workers have found that xDNA<sup>1e</sup> and yDNA<sup>2a</sup> have higher melting points than natural DNA (B-DNA) and that both x-<sup>1b</sup> and y-bases<sup>2a</sup> have stronger stacking interactions than the natural bases. Recent theoretical studies have also found that the x-bases stack more strongly than the natural bases.<sup>6</sup> All these results suggests that it is likely that xDNA and yDNA have

\* Corresponding author. E-mail: fuentescabma@ornl.gov.

<sup>†</sup> Oak Ridge National Laboratory.

<sup>‡</sup> Wrocław University of Technology.

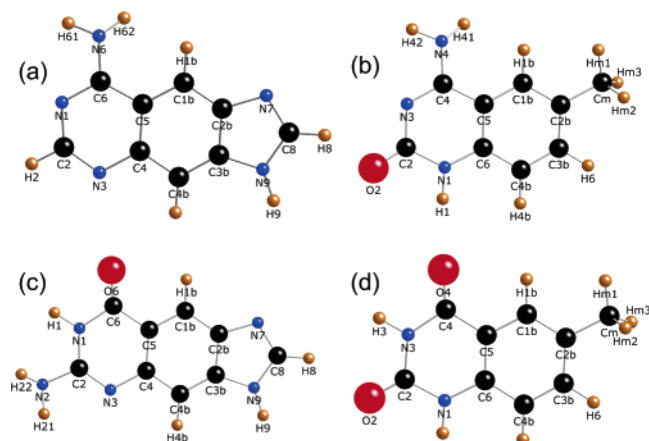


**Figure 2.** Size-expanded x-bases: (a) xA; (b) xC; (c) xG; (d) xT. Color code: oxygen, red; carbon, black; nitrogen, blue; hydrogen, maroon.

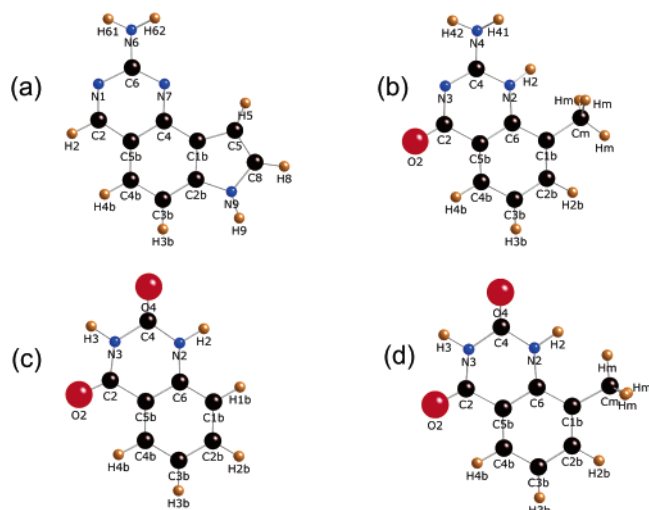


**Figure 3.** Size-expanded y-bases: (a) yA; (b) yC; (c) yT; (d) yT-methyl. Color code: oxygen, red; carbon, black; nitrogen, blue; hydrogen, maroon.

smaller HOMO–LUMO gaps than natural duplexes, and this has motivated us to start a program aimed at elucidating the electronic properties of xDNA and yDNA. But because there is a limited amount of structural experimental data on these duplexes (only one duplex has been investigated with NMR<sup>1d</sup>), it seems wise to focus at first on isolated bases.

Here, we extend our research on size-expanded bases by presenting *ab initio* results on the structural and electronic properties of y-bases. Our objective is 2-fold. First, we wish to verify whether size-expanded bases have, in general, smaller HOMO–LUMO gaps than natural bases. And second, we want to extract *ab initio* structural information useful for generating force fields, because with these force fields it will be possible to obtain reliable models for xDNA and yDNA.

The y-bases that have been synthesized so far are yA, yC, yT-methyl,<sup>7a</sup> and yT, and they are shown in Figure 3. Experimental results on the base yG are not available because it has a more stable tautomer.<sup>7b</sup> We call this tautomer yG-t2, and both yG and yG-t2 are shown in Figure 4a,b, respectively. Figure 4c,d shows the bases yI and yI-t2 (I stands for inosine). Presently, we report results for yA, yC, yG, yG-t2, yT-methyl, and yT. To understand why yG is unstable, we also report our investigation of the bases yI and yI-t2.<sup>7c</sup>

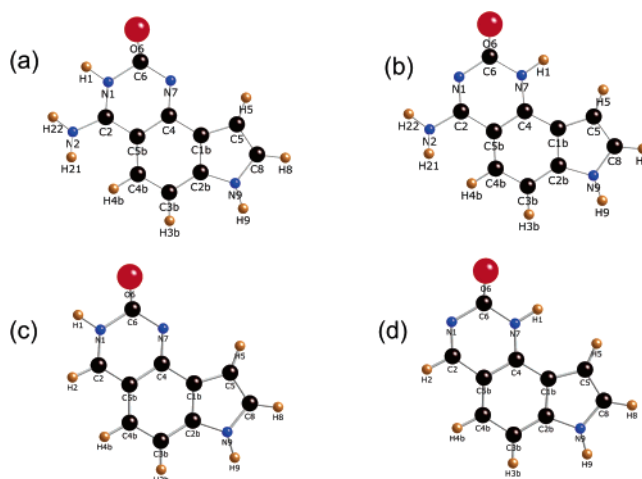


**Figure 4.** Bases used to investigate the instability of yG: (a) yG; (b) yG-t2, a tautomer of yG; (c) yI, which stands for an inosine y-mimic; (d) yI-t2, a tautomer of yI. Color code: oxygen, red; carbon, black; nitrogen, blue; hydrogen, maroon.

## Materials and Methods

The NWChem suite of programs was used for all calculations reported.<sup>8</sup> Optimized geometries were obtained at the MP2/6-31G\*\* level. All chemical structures were relaxed without symmetry restrictions. For the bases yA, yG, and yG-t2, the initial configuration had the two hydrogen atoms of the amino group in a plane different from that occupied by the rest of the atoms. This is done to ensure that the optimized structure is nonplanar, which is known to be more stable than the planar one.<sup>9,10</sup> For yC, the optimized configuration was always nonplanar independent of the initial configuration used.

The electronic properties of the ground-state of each base were obtained using both Hartree–Fock and density-functional theory, with the basis set 6-31G\*\*. To ensure the reliability of our results, different functionals were used for the exchange–correlation potential. These functionals are the local-density and generalized-gradient approximation, LDA<sup>11</sup> and GGA (PW91),<sup>12</sup> respectively, and the hybrid form B3LYP.<sup>13</sup>

For consistency, we previously employed the same methodology to investigate the natural bases A, C, G, and T. Both the structural and electronic properties agreed well with other studies.<sup>5</sup>

## Results

**Structural Properties.** In this section, we discuss the planarity of the amino groups and aromatic rings, and the reasons why yG is unstable.

Originally, it was believed that the natural bases were perfectly planar. This view started to change when Leszczynski<sup>9</sup> and Šponer and Hobza<sup>10</sup> presented high-level *ab initio* calculations, suggesting that the amino groups of the natural bases acquire a pyramidal configuration. In this configuration, both hydrogen atoms of the amino group are pointing out of the plane in one direction, while the nitrogen is also out of the plane, but in the opposite direction. In particular, Šponer and Hobza<sup>10</sup> found that A showed a symmetric pyramidalization (i.e., the hydrogen atoms of the amino group are bent out of the plane by a similar amount). On the other hand, C and G showed an asymmetric pyramidalization, which was explained in terms of a repulsion effect introduced by the hydrogen atoms close to the amino groups (these atoms are H5 for C and H1 for G, see Figure 1b,c).

**TABLE 1: Nonplanarity of the Amino Groups as Calculated by the Torsion Bond Angles (in deg) for the Optimized Structures of the y-Bases<sup>a</sup>**

bond	angle	bond	angle
A			
H61–N6–C6–N1	17.75	H62–N6–C6–C5	–19.77
xA			
H61–N6–C6–N1	–13.75	H62–N6–C6–C5	34.98
yA			
H61–N6–C6–N1	23.42	H62–N6–C6–C5	–21.37
C			
H42–N4–C4–N3	–13.80	H41–N4–C4–C5	25.47
xC			
H42–N4–C4–N3	–12.09	H41–N4–C4–C5	34.18
yC			
H42–N4–C4–N3	9.47	H41–N4–C4–C5	–43.24
G			
H22–N2–C2–N1	–42.23	H21–N2–C2–N3	12.09
xG			
H22–N2–C2–N1	–45.49	H21–N2–C2–N3	10.46
yG			
H22–N2–C2–N1	–23.38	H21–N2–C2–C5b	25.67
yG-t2			
H22–N2–C2–N1	–12.57	H21–N2–C2–C5b	35.29

<sup>a</sup> For comparisons purposes,<sup>14</sup> we also show results on the nonplanarity of the amino groups for the natural and x-bases.<sup>5</sup> It should be noted that when MP2/6-31G\*\* is used, the non-planarity is somewhat exaggerated.<sup>15</sup>

In Table 1, we have collected our results concerning the nonplanarity of the amino groups of the natural, x-, and y-bases. One notices that asymmetrical pyramidalization and repulsion are correlated. For example, xA has a pronounced asymmetrical pyramidalization due to H1b (see Figure 2a); whereas, A and yA have a similar degree of asymmetry because the local configuration around their amino group is also similar (see Figure 1a and Figure 3a). C, xC, and yC, have all an asymmetrical pyramidalization due to the atoms H5, H1b, and H2, respectively (see Figure 1b, Figure 2b, and Figure 3b). However, the correlation seems to not hold for G, xG, and yG: although all these bases have hydrogen atoms close to their amino groups (Figure 1c, Figure 2c, and Figure 4a), only G and xG show an asymmetrical pyramidalization. Further inspection reveals that yG's amino group does not show asymmetry because it has hydrogen atoms (i.e., H1 and H4b) placed on each one of its sides (see Figure 4a). The hydrogen atoms repel both sides of the amino group, and this leads to a symmetrical pyramidalization. As a contra-example, it is instructive to analyze the pyramidalization of yG-t2 because its amino group has only one hydrogen atom nearby (i.e., H4b; see Figure 4b). In this case, one would expect an asymmetrical pyramidalization, with the bending being more pronounced for the bond H21–N2–C2–C5b. This is confirmed in Table 1, suggesting once again that there is a correlation between repulsion and asymmetrical pyramidalization of the amino groups.

Consistent with Šponer and Hobza,<sup>10</sup> we found that the aromatic rings of the natural bases showed a negligible nonplanarity.<sup>5</sup> However, the aromatic rings of the x-bases showed a more pronounced nonplanarity.<sup>5</sup> To reach this conclusion, we compared torsion angles in the natural and x-bases. We performed this comparison by associating the atoms into subgroups and introducing several assumptions. This approach was reasonable because the x-bases can be simply considered as a fusion between benzene and a natural base. For example, xA has four carbon and two hydrogen atoms more

**TABLE 2: Nonplanarity of the Aromatic Rings for the Natural, x-, and y-Bases<sup>a</sup>**

base	first	second	third
A	1.66	1.32	
xA	16.92	8.48	1.51
yA	7.47	13.7	3.04
C	1.87		
xC	22.43	5.29	
yC	23.21	11.37	
G	6.25	1.10	
xG	10.83	9.75	1.52
yG	18.04	20.64	3.91
T	1.87		
xt	0.33	0.67	
yT	0.00	0.00	
yT-methyl	0.00	0.00	

<sup>a</sup> The values were obtained by adding the absolute value of all the torsion angles in each aromatic ring. The angles are given in degrees. First, second, and third refers to the aromatic ring in each base ordered from left to right as shown in Figures 1–4. For example, for the yA base, the first and second ring are six-membered rings, whereas the third is a five-membered ring. For the natural and x-bases, results were taken from ref 5.

than A; these atoms can be seen as belonging to the extra benzene ring that in making xA was fused to A. But the y-bases cannot be simply considered as a fusion between benzene and a natural base, and so analogous comparisons are complicated. (For example, yA has one nitrogen atom less than A, and this cannot be seen as a consequence of having fused A with a benzene ring.) Then, to make comparisons, we focus on one aromatic ring at a time and compare the sum of the torsion angles for each ring.

In Table 2, we present the sum of the absolute values of the torsion angle in each aromatic ring. One observes that both x- and y-bases are less planar than the natural bases. The only exceptions are yT and yT-methyl. This is most likely due to the fact that, for these two bases, the states with planar aromatic rings are metastable, and the optimization procedure was not able to find a more stable state. (A complete list of the torsion angles for the canonical-like y-bases is shown in the Supporting Information; a complete list of the torsion angles for the x- and natural bases is included in the Supporting Information of ref 5.)

As mentioned in the Introduction, experimental results are not available on yG because it has a more stable tautomer (i.e., yG-t2).<sup>7b</sup> This tautomer is, in a sense, undesired because its structure is not compatible with Watson–Crick base pairing. For example, the dimer C–G (or C–yG, if yG were to be stable) has three hydrogen bonds, whereas the dimer C–yG-t2 would have only two hydrogen bonds, which could render it less stable. It is interesting then to understand the origin of yG instability, in the hope that these studies could help designing a stable yG-mimic.

Ab initio calculations show that yG is about 13 kcal/mol less stable than the tautomer yG-t2, which we argue is due to a combination of two effects: yG has a Coulombic repulsion that involves the amino group, and yG is less aromatic than yG-t2. In yG there is a Coulombic repulsion between the H22 atom of the amino group and the atom H1 (see Figure 4a). This repulsion, which is absent in yG-t2 (see Figure 4b), should make yG less stable than yG-t2. Next, we refer to the aromaticity of yG and yG-t2 and specifically to the aromaticity of their benzene rings.

In going from yG to yG-t2, there is a migration of the H1 atom from the N1 location to the N7 location. This migration is accompanied by a switch of adjacent double bonds, which



**TABLE 3: Bond Lengths (in Å) for Bonds between the Atoms of the Extra Benzene Ring, and for the Bond C2–C5b, of the Bases yG, yG-t2, yI, and yI-t2<sup>a</sup>**

base	C5b–C4	C4–C1b	C1b–C2b	C2b–C3b	C3b–C4b	C4b–C5b	C2–C5b	HOMA
yG	1.437	1.429	1.406	1.415	1.371	1.432	1.401	0.750
yG-t2	1.399	1.412	1.414	1.405	1.379	1.419	1.452	0.780
Δ	0.038	0.017	−0.008	0.01	−0.008	0.013	−0.051	
yI	1.447	1.431	1.406	1.421	1.366	1.436	1.379	0.732
yI-t2	1.400	1.411	1.416	1.408	1.377	1.419	1.434	0.795
Δ	0.047	0.02	−0.01	0.013	−0.011	0.017	−0.055	

<sup>a</sup> Δ is defined as the difference between the length of the same bond in yG (yI) and yG-t2 (yI-t2). The last column shows the HOMA index of the molecule.

can be observed in detail in Table 3. In this table we have collected the bond lengths for all atoms of the extra benzene ring and also the length of the bond C2–C5b that is outside the benzene ring. The variable Δ quantifies the change in bond length that occurs when yG becomes yG-t2. A positive Δ means a decreasing in bond length, and a negative one means the opposite. One can see that the largest values for Δ occur for the bonds C2–C5b and C5b–C4 and that the Δ values for the bonds C4–C1b, C2b–C3b, C4b–C5b, C1b–C2b, and C3b–C4b are less significant. This means that C2–C5b and C5b–C4 are the bonds that change the most in going from yG to yG-t2. Specifically, the bond C2–C5b is shorter in yG than in yG-t2, and the bond C5b–C4 is larger in yG than in yG-t2. These changes in bond length are consistent with the switching of adjacent double bonds characteristic of tautomerism.

As a consequence of this bond switching, yG-t2 is more aromatic than yG, and this is specially true for their benzene rings. To reach this conclusion, we have quantified the aromaticity of yG and yG-t2 and their rings by means of the harmonic oscillator model of aromaticity (HOMA) index.<sup>16</sup> The HOMA is one of the most widely used indices to quantify the aromaticity of molecules, and it is given by the following expression:

$$\text{HOMA} = 1 - \frac{\alpha_{\text{CC}} \sum_i (R_{\text{opt}}^{\text{CC}} - R_i^{\text{CC}})^2}{n} - \frac{\alpha_{\text{CN}} \sum_i (R_{\text{opt}}^{\text{CN}} - R_i^{\text{CN}})^2}{n}$$

where  $n$  is total number of bonds considered;  $\alpha_{\text{CC}}$  and  $\alpha_{\text{CN}}$  are empirical constants with values of 257.7 and 93.2 for C–C and C–N bonds, respectively;  $R_{\text{opt}}^{\text{CC}}$  and  $R_{\text{opt}}^{\text{CN}}$  are 1.388 and 1.334 Å, and they are the optimal values for C–C and C–N bonds in a fully aromatic system, respectively;  $R_i$  is a bond length within the molecule that is being studied. HOMA varies between 0 and 1, which are the values it takes for a model nonaromatic and fully aromatic system, respectively.

The last column of Table 3 shows the HOMA index for yG and yG-t2, and one can see that yG-t2 is slightly more aromatic than yG. The different aromaticity of these molecules is clearer when one compares the HOMA index for their fragments. Figure 5, panels a and b, shows the structures of yG and yG-t2 with the HOMA index for their fragments. One can see that the extra benzene ring of yG-t2 is much more aromatic than that of yG and that the aromaticity of this fragment is the one that changes the most in going from yG to yG-t2. We conclude that yG-t2 is more aromatic than yG due mostly to the larger aromaticity of its extra benzene. Finally, we reason that the larger aromaticity of yG-t2 contributes to make it more stable than yG.

To gain increased insight into the difference in stabilities between yG and yG-t2, we investigate the base yI, shown in Figure 4c, and its tautomer yI-t2, shown in Figure 4d.<sup>7c</sup> Ab initio calculations show that yI is about 7 kcal/mol less stable than yI-t2. We suggest that this energy difference is the result of a different aromaticity. Indeed, Table 3 and Figure 5c,d show that

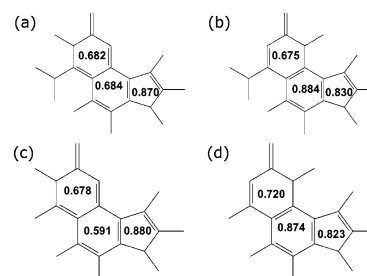


**Figure 5.** Structures of yG, yI, and their tautomers yG-t2 and yI-t2, respectively. These plots show which bonds are single and which are double. They also indicate the HOMA index for each ring; the HOMA index for the whole molecule is given in Table 3: (a) yG; (b) yG-t2; (c) yI; (d) yI-t2.

(i) the switch of adjacent double bonds that takes place in going from yI to yI-t2 is completely similar to the one that takes place in going from yG to yG-t2 and (ii) yI-t2 is more aromatic than yI due mostly to the larger aromaticity of its extra benzene ring.

The results on the energy difference between yI and yI-t2 also serve to give a qualitative idea as to the relative importance that the Coulombic repulsion associated with the amino group has in destabilizing yG. For example, if one assumes that in destabilizing yG, the Coulombic repulsion and aromaticity effects act independently, then one would think that by removing the amino group we will be left only with an aromaticity destabilizing energetic effect. This effect can be quantified from yI, for this base is just like yG except without the amino group. Then, since the aromaticity in yI accounts for 7 kcal/mol, the Coulombic repulsion in yG accounts for a destabilization energy of  $13 - 7 = 6$  kcal/mol. This is of course an upper limit, for in obtaining it we assumed that in destabilizing yG, the Coulombic repulsion and aromaticity effects can be decoupled.

**Electronic Properties.** In 1962, Eley and Spivey put forward the idea that natural DNA could conduct electricity.<sup>17</sup> They argued that the interactions between stacked bases, in particular the interactions between  $\pi_z$  electrons perpendicular to the plane of the bases, could promote charge transport along DNA. We are interested in xDNA and yDNA because they might also conduct electricity, and are motivated by the following facts. First, Kool and co-workers have found that xDNA<sup>1e</sup> and yDNA<sup>2a</sup> have higher melting points than B-DNA, and that both x-<sup>1b</sup> and y-bases<sup>2a</sup> have stronger stacking interactions than the natural bases. Huertas et al. have also carried out theoretical studies on xDNA duplexes and found that the x-bases stack more strongly than natural bases.<sup>6</sup> Second, we have found that the x-bases have smaller HOMO–LUMO gaps than natural bases.<sup>5</sup> These facts point to the possibility that xDNA and yDNA duplexes could have smaller band gaps than B-DNA, which could make them useful for molecular wire applications. To obtain further proof, one needs to investigate the electronic properties of xDNA and yDNA, for example, with the same ab initio techniques that have been used to study the electronic properties of

**TABLE 4: HOMO and LUMO Orbital Energies and HOMO–LUMO Gap for the y-Bases As Calculated with LDA/6-31G\*\*<sup>a</sup>**

base	HOMO	LUMO	gap
yA	1.21	4.09	2.89
yC	0.90	4.10	3.19
yG	1.46	3.95	2.50
yT	0.00	3.55	3.55
yT-methyl	0.15	3.64	3.49
A	0.56	4.44	3.88 (3.84)
C	0.50	4.14	3.63 (3.64)
G	0.81	4.81	4.00 (3.85)
T	0.10	3.97	3.87 (3.76)
xA	0.72	3.62	2.90
xC	0.58	3.62	3.04
xG	0.89	4.05	3.16
xT	0.22	3.62	3.40
yG-t2	0.96	4.19	3.23
yI	1.13	3.35	2.22
yI-t2	0.73	3.63	2.90

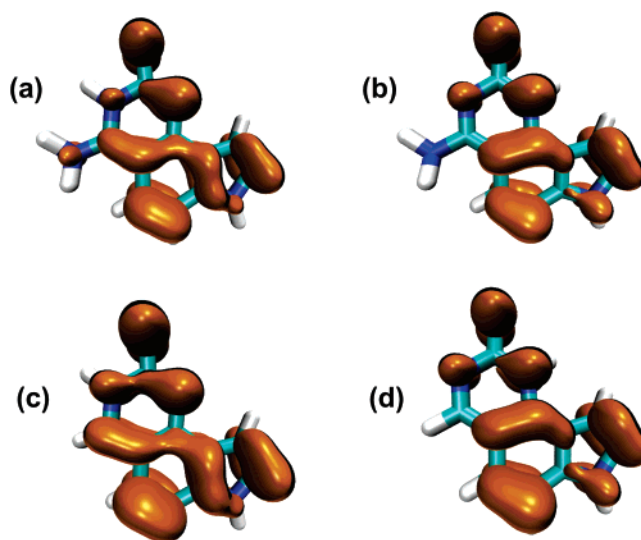
<sup>a</sup> The energies, in eV, are given relative to yT's HOMO. For comparisons purposes, we also show the HOMO and LUMO orbital energies and HOMO–LUMO gap for the natural and x-bases.<sup>5</sup> In parentheses, we have included the HOMO–LUMO gaps of the natural bases obtained in ref 19, which used the methods of plane-wave basis, ultrasoft pseudopotentials, and GGA approximation to the exchange–correlation functional.

B-DNA.<sup>18</sup> But given the limited amount of experimental data on xDNA and yDNA, it is wise to begin with smaller models (i.e., isolated bases). This is the reasoning that led us to study the electronic properties of the x-bases, and the same reasoning leads us to extend this work by studying the electronic properties of the y-bases.

Table 4 gives the HOMO–LUMO gaps of the y-bases, natural, and x-bases. All the calculations were done with LDA.<sup>11</sup> We have confidence in the results presented here because the HOMO–LUMO gaps of the natural bases are in good agreement with previous studies,<sup>19</sup> and the trends we observe are independent of the theoretical method used. (In the Supporting Information, we include the HOMO–LUMO gaps obtained with Hartree–Fock, GGA, and B3LYP.)

When comparing HOMO and LUMO energetics for natural, x- and y-bases, and for making comparisons more straightforward, it is useful to limit oneself to the canonical-like forms (e.g., A, C, G, T, xA, xC, xG, xT, yA, yC, yG, yT, and yT-methyl). As such, we have decided to leave out of this discussion the bases yG-t2, yI, and yI-t2. Later on, when discussing HOMO–LUMO gaps, these bases will be included in the discussion. In Table 4, it is observed that the HOMO states of natural and x- and y-bases show the same energy ordering. For the natural bases, T has the lowest HOMO, followed by C, A, and G. The same is true for x- and y-bases (the HOMO of yT-methyl being smaller and larger than those of yC and yT, respectively). The ordering for the LUMO state is not the same for all these bases. For the natural bases, T has the lowest LUMO, followed by C, A, and G. For the x-bases, the LUMOs of xT, xC, and xA have practically the same energy, and xA has the highest LUMO. For y-bases, yT has the lowest LUMO, followed by yT-methyl, yG, yA, and yC, the LUMO of the last two having practically the same energy.

When comparing HOMO–LUMO gaps, one notices the following. yC and yT both have larger and smaller HOMO–LUMO gaps than their x- and natural congeners, respectively. The HOMO–LUMO gap of yA and xA are practically the same and smaller than that of A. The HOMO–LUMO gap of yG is 0.66 and 1.5 eV smaller than those of xG and G, respectively.

**Figure 6.** Electronic charge densities for the HOMO states of (a) yG; (b) yG-t2; (c) yI; (d) yI-t2.

In fact, among all canonical-like forms bases, yG is the base that has the smallest HOMO–LUMO gap. Why? Now, it is instructive to include in this discussion the HOMO–LUMO gaps of the bases yG-t2, yI and yI-t2.

The base yG has a HOMO–LUMO gap that is 0.73 eV smaller than that of yG-t2, which is remarkable given that these two bases are tautomeric pairs and differ only by the position of one hydrogen atom. The 0.73 eV difference in the HOMO–LUMO gap is comprised of a 0.5 eV increase of the HOMO state of yG with respect to that of yG-t2 and a 0.23 decrease of the LUMO state of yG with respect to that of yG-t2. Therefore, the dominate effect is a dramatic 0.5 eV increase of the HOMO state of yG. We believe the reason for the very different HOMO–LUMO gaps between these bases to be directly related to differences in their aromaticity. Specifically, the aromatic stability of yG-t2 is much greater than yG. This can be directly observed in Figure 6a,b, where we have plotted the charge-densities for the HOMO orbitals of yG and yG-t2. Clearly, the HOMO of yG-t2 is more concentrated over the benzene ring, whereas the HOMO of yG extends outside of this ring following the path C2–C5b–C4–C1b–C2b–N9.

In a directly analogous manner, we have also found that the HOMO–LUMO gap of yI is very small as compared to that of yI-t2, in particular 2.22 versus 2.90 eV, respectively. This is also explained by the much larger aromatic stability of yI-t2. Indeed in Figure 6c,d one can see that the HOMO of yI-t2 is more concentrated over the benzene ring, as compared to the HOMO of yI.

For the purposes of our present considerations, it is unfortunate that yG, having such a small HOMO–LUMO gap, is unstable. This is because a hypothetical yDNA such as poly(yG)·poly(C), could have a small HOMO–LUMO gap. One wonders then if our results concerning the instability of yG in gas phase change when solvation is considered. For example, Huertas et al.<sup>6</sup> have studied the tautomeric forms of the x-bases, and they have found that in gas-phase xC is not stable in a canonical-like form, whereas it is stable in solvent. Furthermore, our results also make one wonder whether yA, yC, yT, and yT-methyl are stable in the canonical-like form or, as yG, have tautomeric forms that are more stable. All these observations suggest the need for further studies on the y-bases (for example, studies on their tautomeric forms), to elucidate whether yDNA duplexes could have molecular wire applications.

## Conclusions

Size-expanded bases (i.e., x- and y-bases) can be very useful in several biological contexts, from probing the DNA–protein interactions to developing biosensor assays. Additionally, we are interested in the possibility that size-expanded DNAs (i.e., xDNA and yDNA duplexes) could function as nanowires. To answer this question, it is necessary to investigate both the structure and electronic properties of these duplexes. But the limited amount of experimental structural information on these duplexes first requires development of reliable theoretical models. To this end, it is necessary to obtain information for smaller models (i.e., isolated bases and base-pairs) and then to use this information to build larger models. Presently, our focus is on the structural and electronic properties of isolated x- and y-bases. In this paper, we investigated the y-bases, and the results we have found complement those we previously obtained for the x-bases. In this general context, one observes the following. Size-expanded bases are less planar than natural bases, and this nonplanarity occurs both in the amino groups and in the aromatic rings. This nonplanarity could restrict the type of force fields that one can choose to perform molecular dynamics of xDNA and yDNA duplexes. In particular, accurate results might require force fields that account for nonplanarity. The ab initio data provided here should be useful for developing such force fields. Size-expanded bases have smaller HOMO–LUMO gaps than natural bases. This result, combined with the experimental higher melting point of xDNA and yDNA duplexes and the stronger stacking interactions between size-expanded bases, suggests an interesting proposition: that these duplexes could have smaller HOMO–LUMO gaps than natural DNA, and so that they might be useful in molecular wire applications. Furthermore, we have found that the HOMO–LUMO gap of yG can be changed dramatically (i.e., can be increased by ca. 0.75 eV, by changing the aromaticity of its extra benzene ring). This suggests that the size-expanded bases have a knob that can be used to modulate the electronic properties of size-expanded duplexes. This knob is their extra benzene ring, which natural bases do not have. In summary, size-expanded not only have smaller HOMO–LUMO gaps than the natural bases but also one might be able to change their structure as to reduce further their HOMO–LUMO gaps. In light on these results, we are intrigued by the possibility that xDNA and yDNA duplexes could have application as molecular wires. We hope that our results will encourage experimentalists to explore the electronic and conductive properties of these duplexes.

**Acknowledgment.** The authors thank Professor Eric T. Kool and Professor F. Javier Luque for many insightful discussions. Work at Oak Ridge National Laboratory (ORNL) was supported by ORNL's Laboratory Directed Research and Development Program (B.G.S.) and by the Center for Nanophase Materials Sciences, sponsored by the Division of Scientific User Facilities, U.S. Department of Energy (USDOE) (M.F.-C., B.G.S., J.C.W.), and used resources of the National Center for Computational Sciences, ORNL, supported by the Office of Science, USDOE (M.F.C., B.G.S., J.C.W.).

**Supporting Information Available:** Atomic coordinates for all the structures investigated and their absolute energies in hartrees, bond lengths, bond angles, dipole moments, and HOMO and LUMO energies. This material is available free of charge at <http://pubs.acs.org>.

## References and Notes

- (1) (a) Liu, H.; Gao, J.; Maynard, L.; Saito, D. Y.; Kool, E. T. *J. Am. Chem. Soc.* **2004**, *126*, 1102–1109. (b) Gao, J.; Liu, H.; Kool, E. T. *J. Am. Chem. Soc.* **2004**, *126*, 11826–11831. (c) Liu, H.; Gao, J.; Kool, E. T. *J. Org. Chem.* **2005**, *70*, 639–647. (d) Liu, H.; Gao, J.; Lynch, S. R.; Saito, Y. D.; Maynard, L.; Kool, E. T. *Science* **2003**, *302*, 868–871. (e) Liu, H.; Gao, J.; Lynch, S. R.; Kool, E. T. *J. Am. Chem. Soc.* **2004**, *126*, 6900–6905. (f) Liu, H.; Gao, J.; Kool, E. T. *J. Am. Chem. Soc.* **2005**, *127*, 1396–1402. (g) Gao, J.; Liu, H.; Kool, E. T. *Angew. Chem., Int. Ed.* **2005**, *44*, 3118–3122.
- (2) (a) Lu, H.; He, K.; Kool, E. T. *Angew. Chem., Int. Ed.* **2004**, *43*, 5834–5836. (b) Lee, A. H. F.; Kool, E. T. *J. Org. Chem.* **2005**, *70*, 132–140. (c) Lee, A. H. F.; Kool, E. T. *J. Am. Chem. Soc.* **2005**, *127*, 3332–3338.
- (3) Kim, T. W.; Delaney, J. C.; Essigmann, J. M.; Kool, E. T. *Proc. Natl. Acad. Sci. U.S.A.* **2005**, *102*, 15803–15808.
- (4) (a) Ding, B.; Sha, R.; Seeman, N. C.; *J. Am. Chem. Soc.* **2004**, *126*, 10230–10231. (b) Seeman, N. C. *Nature* **2003**, *421*, 427–431.
- (5) Fuentes-Cabrera, M.; Sumpter, B. G.; Wells, J. C. *J. Phys. Chem. B* **2005**, *109*, 21135–21139.
- (6) Huertas, O.; Blas, J. R.; Soteras, I.; Orozco, M.; Luque, F. J. *J. Phys. Chem. A* **2006**, *110*, 510–518.
- (7) Kool, E. T. Private communication. (a) Although results for the base yT-methyl have not been published, this base has been synthesized as well. (b) yG-t2 is more stable than yG. (c) As suggested by E. T. Kool.
- (8) (a) Aprà, E.; et al. *NWChem, A Computational Chemistry Package for Parallel Computers, Version 4.7*; Pacific Northwest National Laboratory: Richland, WA, 2005. (b) Kendall, R. A.; Aprà, E.; Bernholdt, D. E.; Bylaska, E. J.; Dupuis, M.; Fann, G. I.; Harrison, R. J.; Ju, J.; Nichols, J. A.; Nieplocha, J.; Straatsma, T. P.; Windus, T. L.; Wong, A. T. *Comput. Phys. Comm.* **2000**, *128*, 260–283.
- (9) Leszczynski, J. *Int. J. Quantum Chem., Quantum Biol. Symp.* **1992**, *Suppl. 19*, 43–55.
- (10) (a) Šponer, J.; Hobza, P. *J. Phys. Chem.* **1994**, *98*, 3161–3164. (b) Hobza, P.; Šponer, J. *Chem. Rev.* **1999**, *99*, 3247–3276.
- (11) (a) Slater, J. C. *Quantum Theory of Molecules and Solids*, Vol. 4; McGraw-Hill: New York, 1974. (b) Vosko, S. J.; Wilk, L.; Nusair, M. *Can. J. Phys.* **1980**, *58*, 1200–1211. (c) Ceperly, D. M.; Alder, B. J. *Phys. Rev. Lett.* **1980**, *45*, 566–569.
- (12) Perdew, J. P.; Chvary, J. A.; Vosko, S. H.; Jackson, K. A.; Pederson, M. R.; Singh, D. J.; Fiolhais, C. *Phys. Rev. B* **1992**, *46*, 6671–6887.
- (13) Becke, A. D. *J. Chem. Phys.* **1993**, *98*, 5648–5652.
- (14) In some cases, the same torsion angles in the natural, x- and y-bases have different signs. For example the torsion angle defined by H61–N6–C6–C1 is positive in A and yA and negative in xA. This difference in sign is caused by the direction in which the hydrogen atoms were bent away from the plane of the aromatic rings in the initial configurations. In this particular example, we initially bent the hydrogen atoms of A (yA) and xA in opposite directions, and the optimization of the structures did not change this fact. Despite this, comparisons can still be made.
- (15) Bludský, O.; Šponer, J.; Leszczynski, J.; Špirko, V.; Hobza, P. *J. Chem. Phys.* **1996**, *105*, 11042–11050.
- (16) (a) Kruszewski, J.; Krygowski, T. M. *Tetrahedron Lett.* **1972**, *13*, 3839–3842. (b) Krygowski, T. M. *J. Chem. Inf. Comput. Sci.* **1993**, *33*, 70–78.
- (17) Eley, D. D.; Spivey, D. I. *Trans. Faraday Soc.* **1962**, *58*, 411–415.
- (18) (a) Wang, H.; Lewis, J. P.; Sankey, O. F. *Phys. Rev. Lett.* **2004**, *93*, 016401-1–016401-4. (b) Lewis, J. P.; Cheatham, T. E.; Starikov, E. B.; Wang, H.; Sankey, O. F. *J. Phys. Chem. B* **2003**, *107*, 2581–2587. (c) de Pablo, P.; Moreno-Herrero, F.; Colchero, J.; Gómez-Herrero, J.; Herrero, P.; Baro, A. M.; Ordejón, P.; Soler, J. M.; Artacho, E. *Phys. Rev. Lett.* **2000**, *85*, 4992–4995.
- (19) Preuss, M.; Schmidt, W. G.; Seino, K.; Furthmüller, Bechstedt, F. *J. Comput. Chem.* **2004**, *25*, 112–122.